Supramolecular and homogeneous electrocatalytic HER properties of new heteroleptic cyanoacetamide dithiolate based Ni(II) tertiary phosphanes: Effect of co-ligand flexibility on electrocatalytic performance

Shreya Srivastava,[a] Daniel Omoding,[a] Aparna Kushwaha,[a] Gabriele Kociok-Köhn,[b]* Sarfaraz Ahmed,[c] Abhinav Kumar[a]*

[a]*Department of Chemistry, Faculty of Science, University of Lucknow, Lucknow 226 007, India.*

Email: abhinavmarshal@gmail.com

[b] Physical Structure Characterization, University of Bath, Claverton Down, Bath, BA2 7AY, UK. Email: chsgk@bath.ac.uk

[c]Department of Pharmacognosy, College of Pharmacy, King Saud University, P.O. Box 2457 Riyadh 11451, Saudi Arabia

Electronic Supplementary Information

Contents in Supporting Information		
S/No.	**Content**	**Page No.**
1	**Fig. S1** FTIR spectrum of **K_2CAM, Ni-1, Ni-2 and Ni-3**	**3**
2	**Fig. S2** ^{1}H NMR spectrum of **K_2CAM**	**3**
3	**Fig. S3** ^{13}C NMR spectrum of **K_2CAM**	**4**
4	**Fig.S4** ^{1}H NMR spectrum of **Ni-1**	**5**
5	**Fig.S5** ^{13}C NMR spectrum of **Ni-1**	**6**
6	**Fig.S6** ^{31}P NMR spectrum of **Ni-1**	**6**
7	**Fig. S7** ^{1}H NMR spectrum of **Ni-2**	**7**
8	**Fig.S8** ^{13}C NMR spectrum of **Ni-2**	**7**
9	**Fig.S9** ^{31}P NMR spectrum of **Ni-2**	**8**
10	**Fig.S10** ^{1}H NMR spectrum of **Ni-3**	**9**
11	**Fig.S11** ^{13}C NMR spectrum of **Ni-3**	**10**
12	**Fig.S12** ^{31}P NMR spectrum of **Ni-3**	**11**
13	**Fig. S13** Results of the Hirshfeld surface analyses for Ni-1, Ni-2 and Ni-3 showing d_{norm}, shape index and curvedness.	**12**
14	**Fig. S14** Total and delineated 2D fingerprint plots for Ni-1, Ni-2 and Ni-3.	**13**
15	**Fig. S15-S17** NCI plots for all Ni-1, Ni-2 and Ni-3	**14-16**

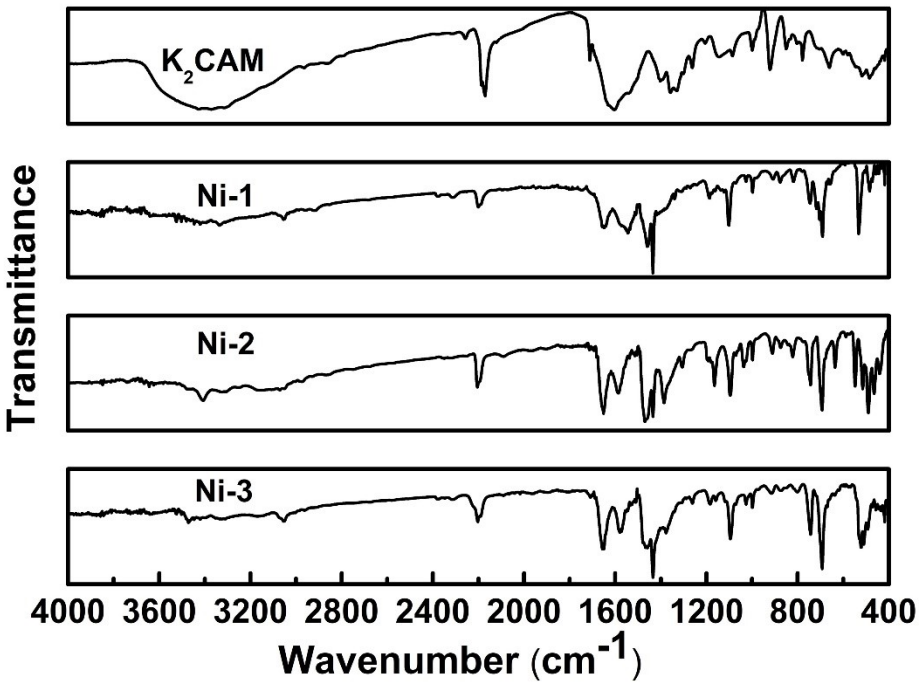

Fig. S1 FTIR spectra of ligand and the complexes.

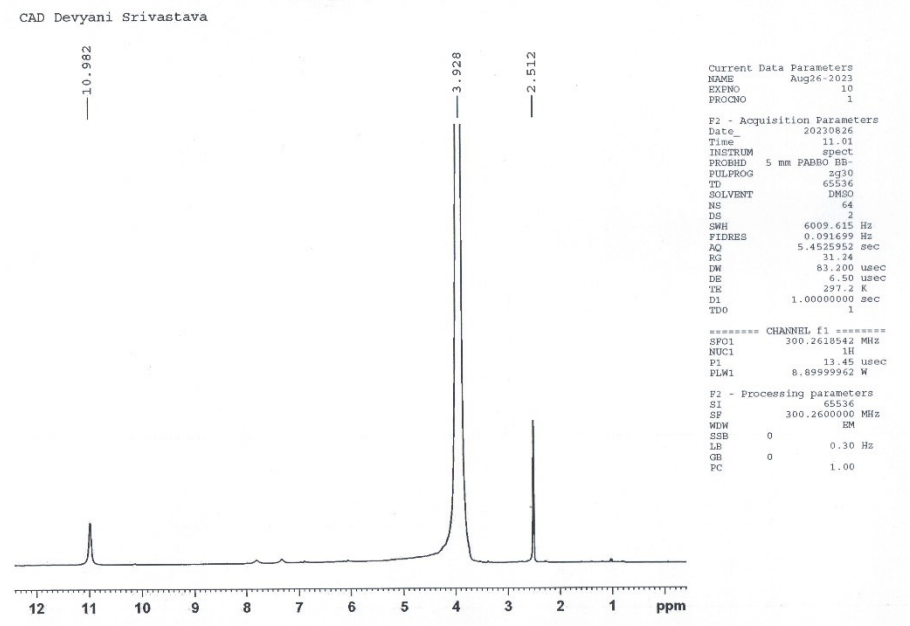

Fig. S2 ^{1}H NMR spectrum of **K_2CAM**

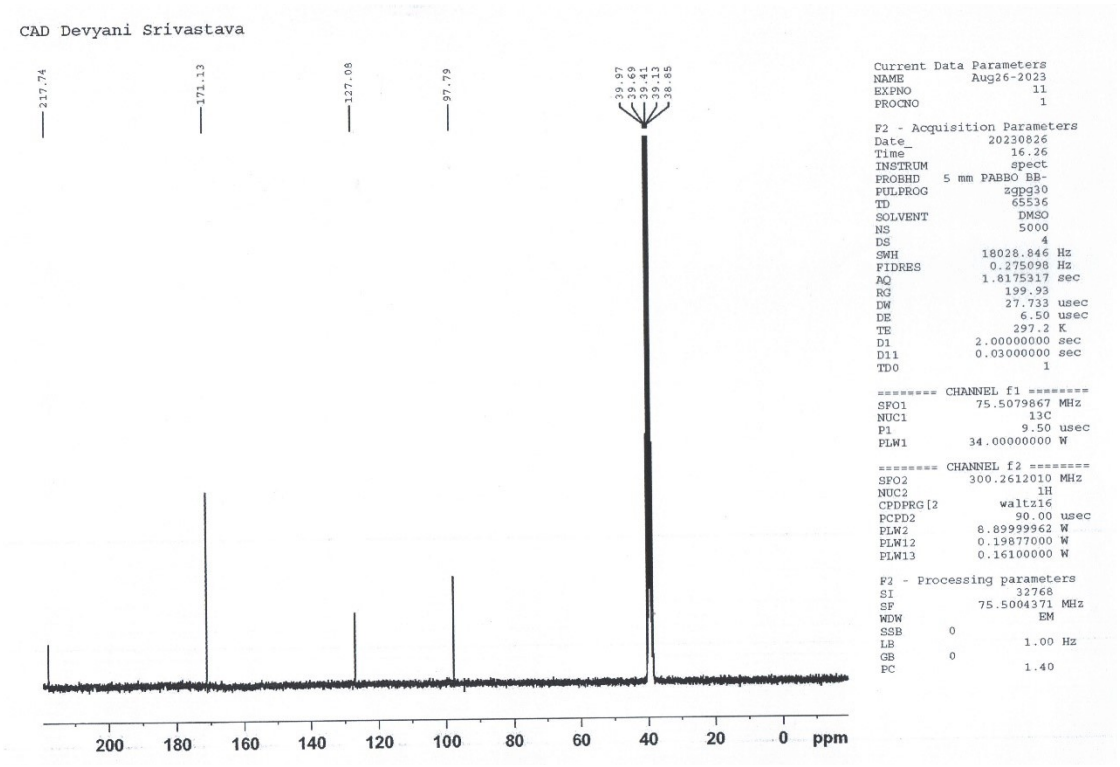

Fig. S3 ^{13}C NMR spectrum of **K_2CAM**

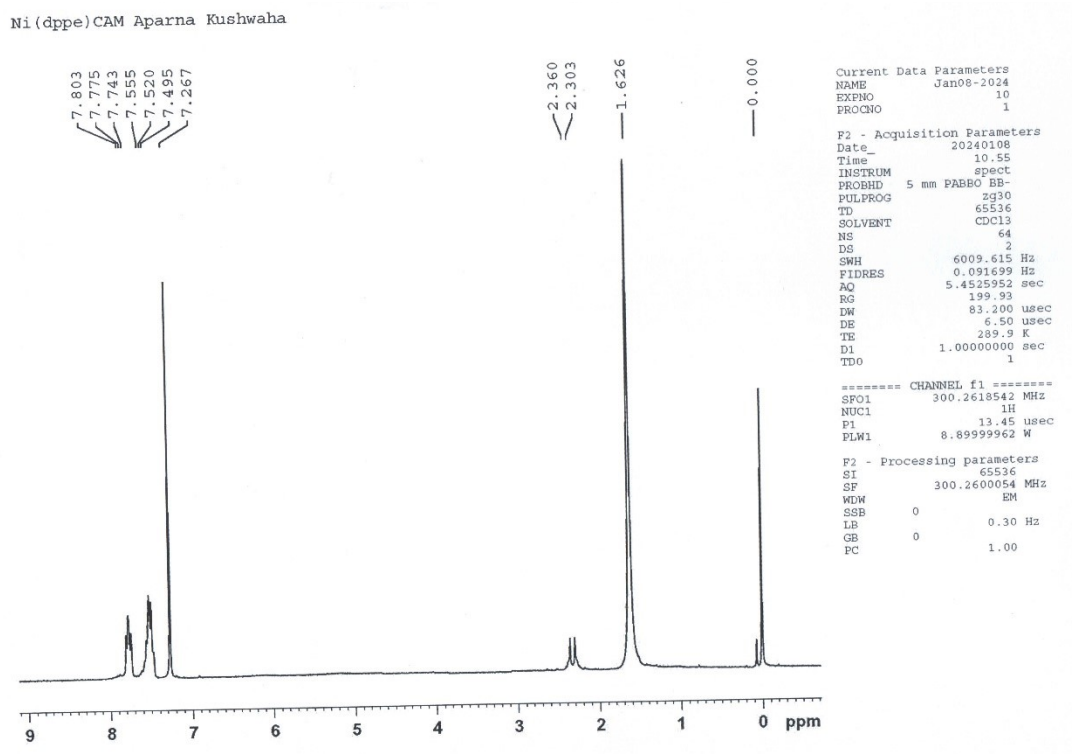

Fig.S4 ^{1}H NMR spectrum of **Ni-1**.

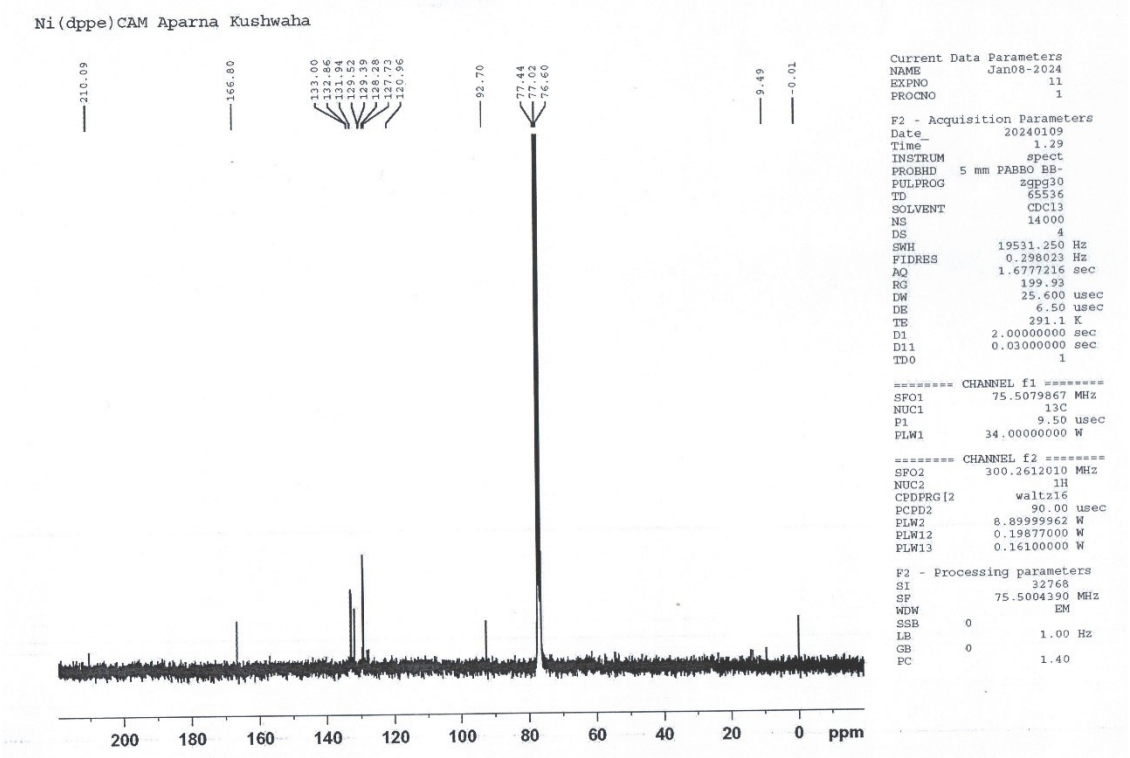

Fig. S5 ^{13}C NMR spectrum of **Ni-1**.

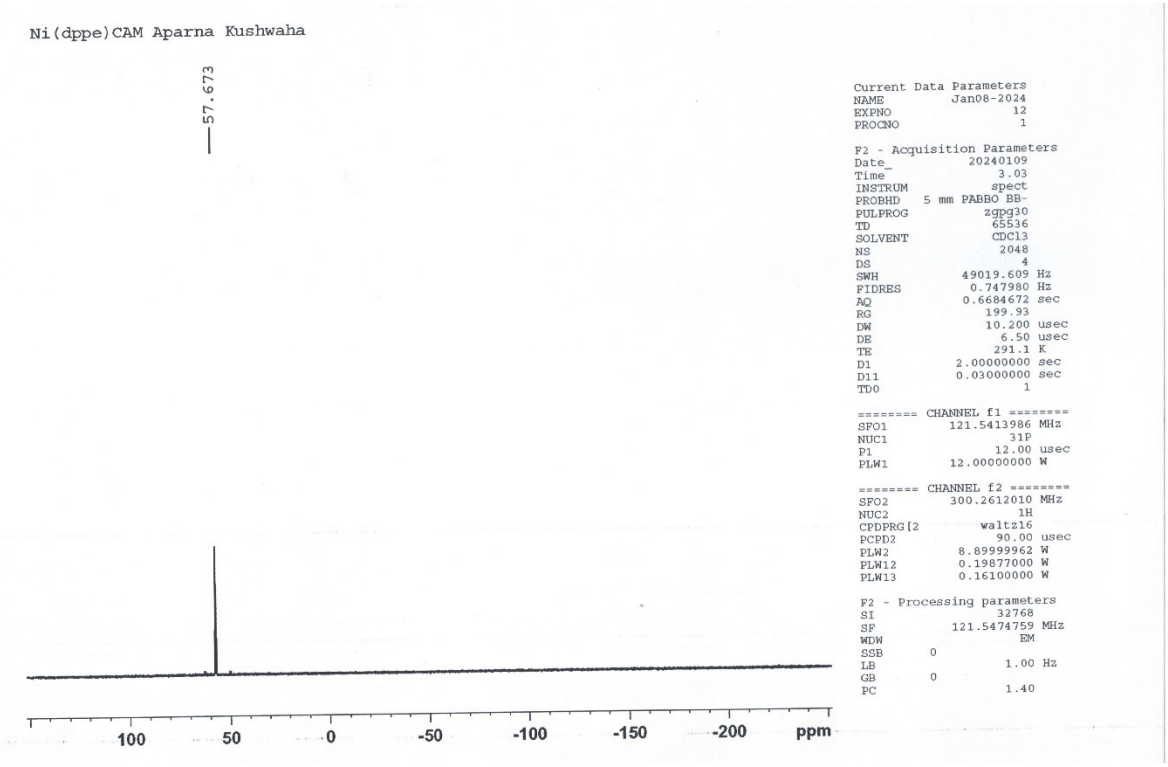

Fig. S6 ^{31}P NMR spectrum of **Ni-1**.

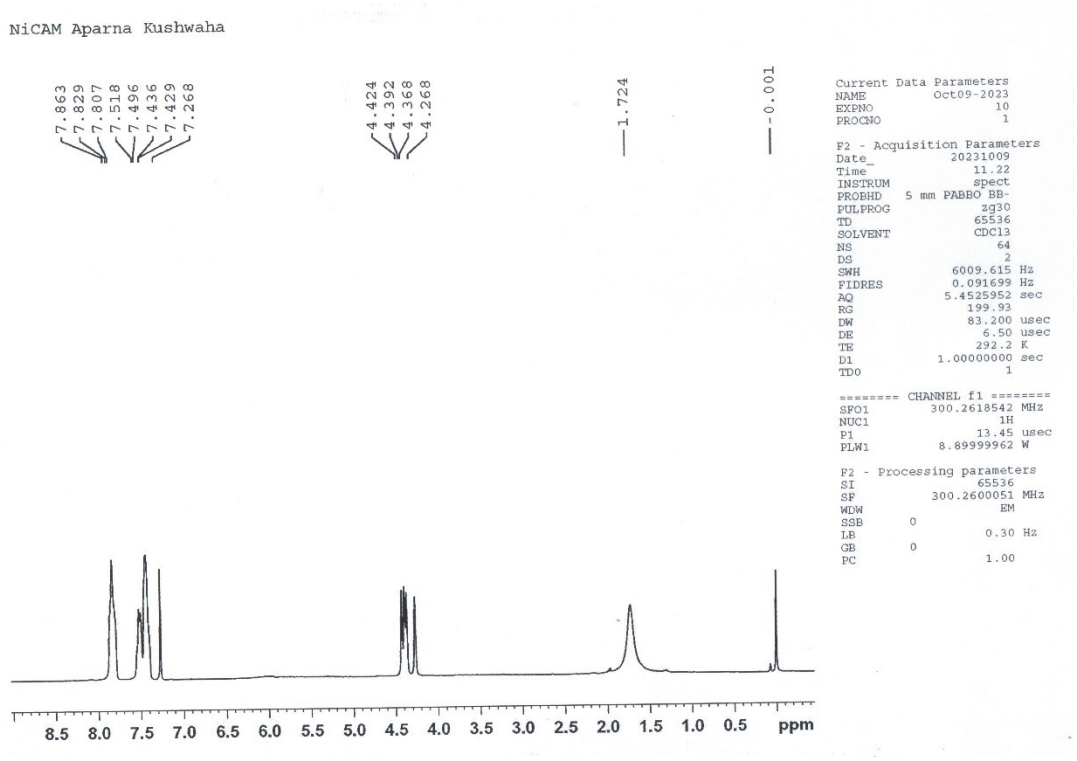

Fig. S7 ^{1}H NMR spectrum of **Ni-2**.

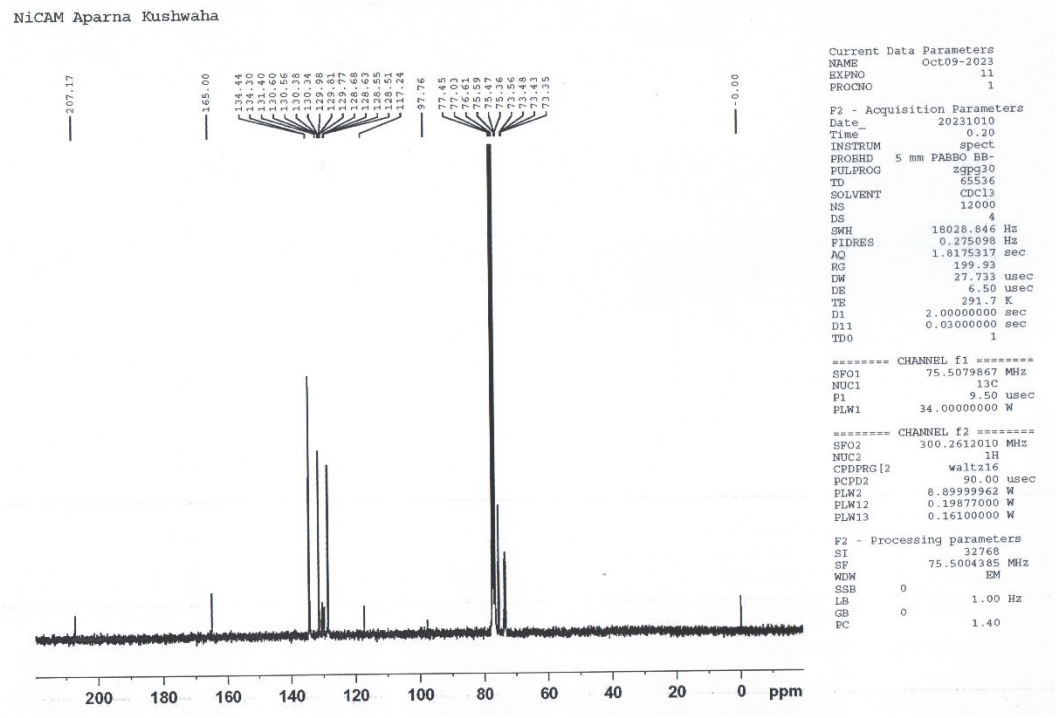

Fig. S8 ^{13}C NMR spectrum of **Ni-2**.

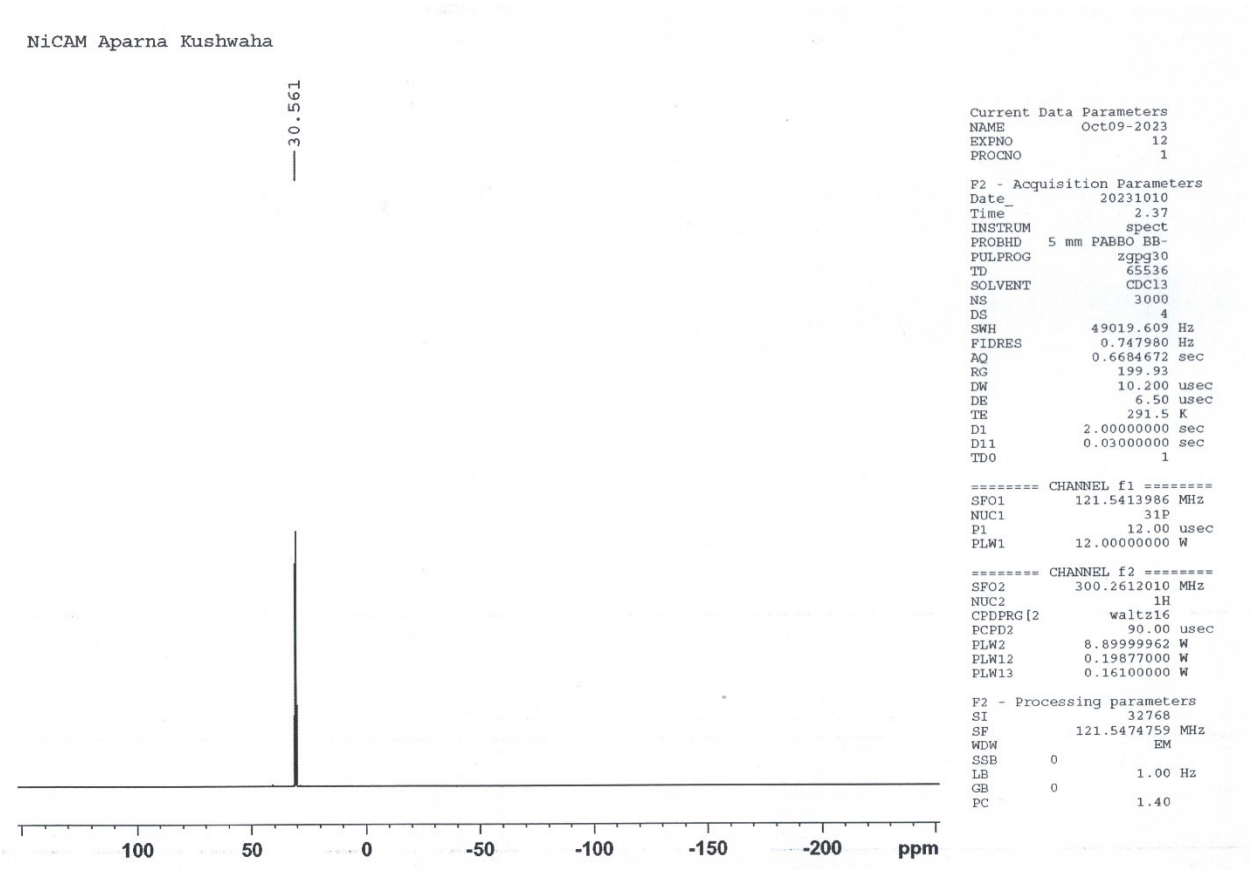

Fig. S9 ^{31}P NMR spectrum of **Ni-2**.

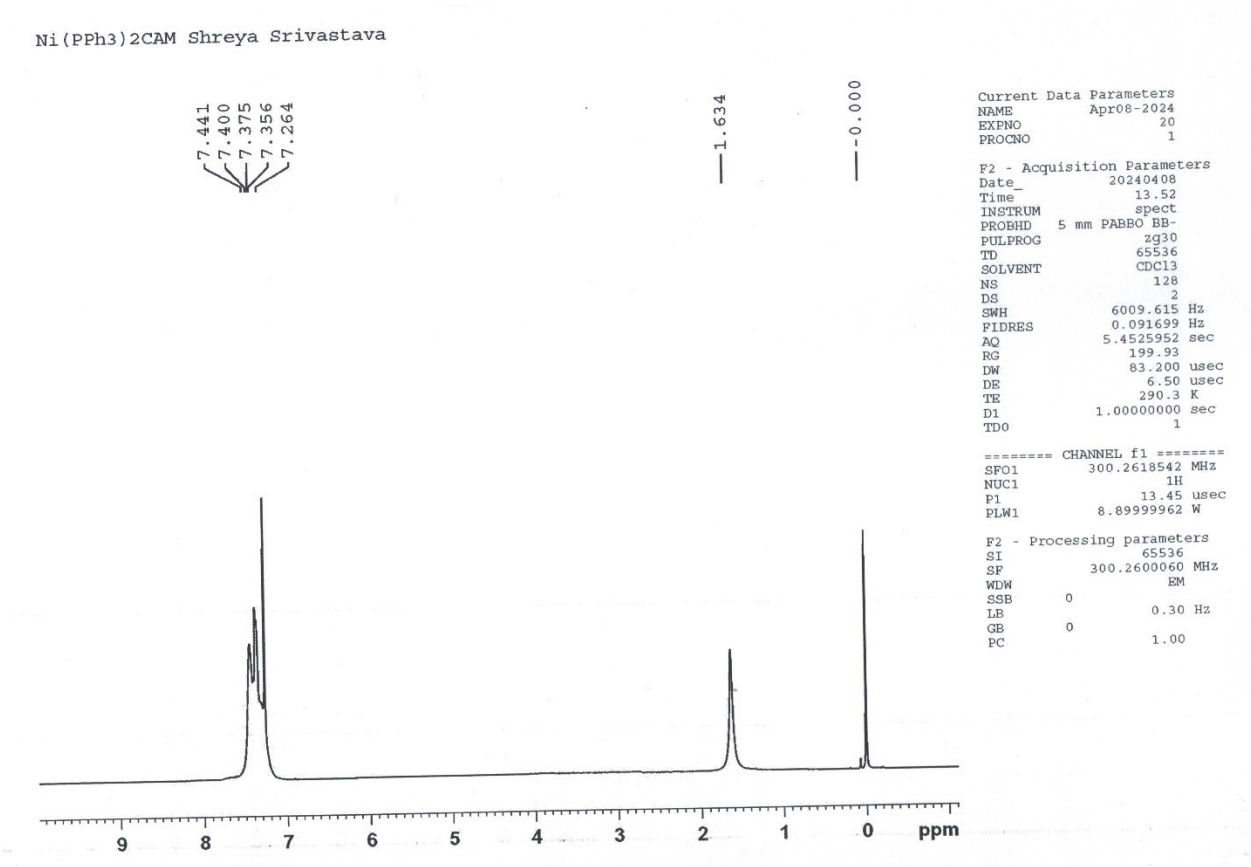

Fig. S10 ^{1}H NMR spectrum of **Ni-3**.

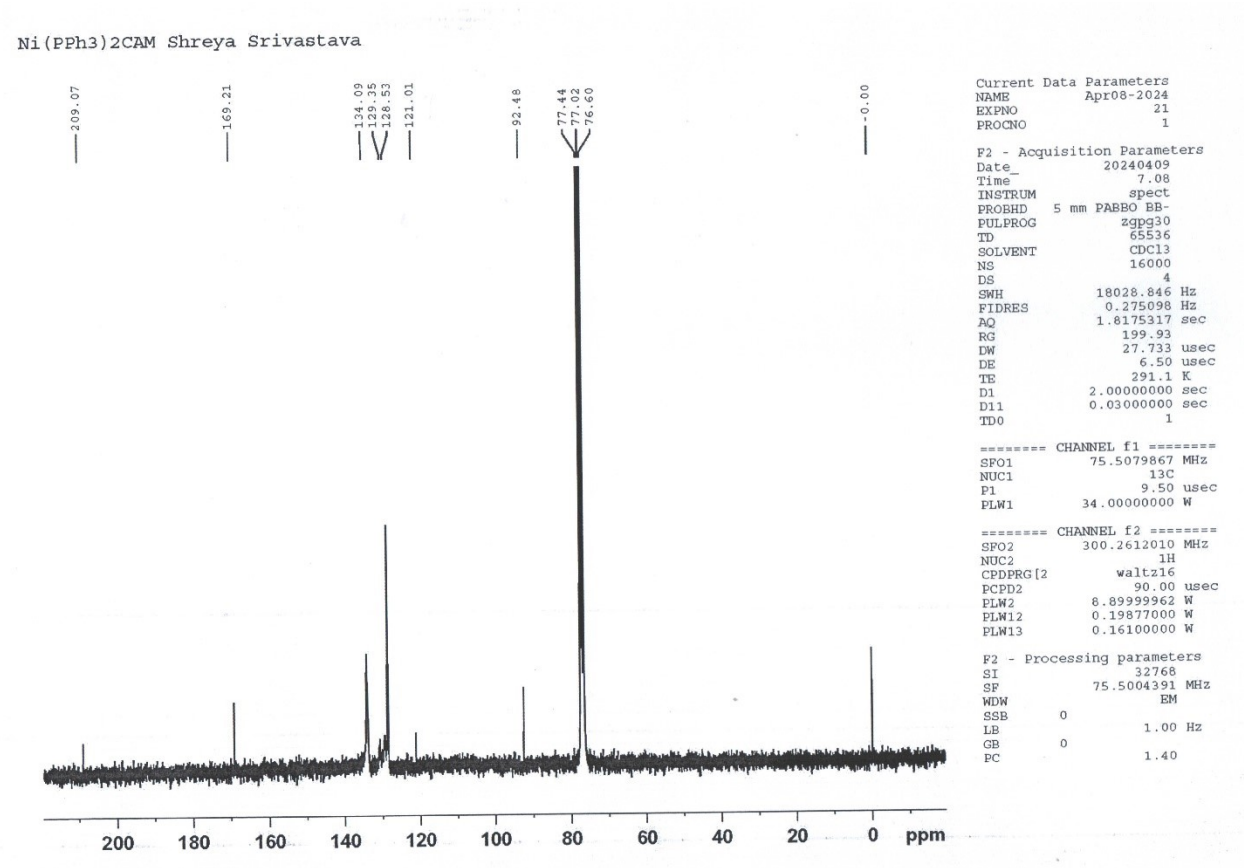

Fig. S11 ^{13}C NMR spectrum of **Ni-3**.

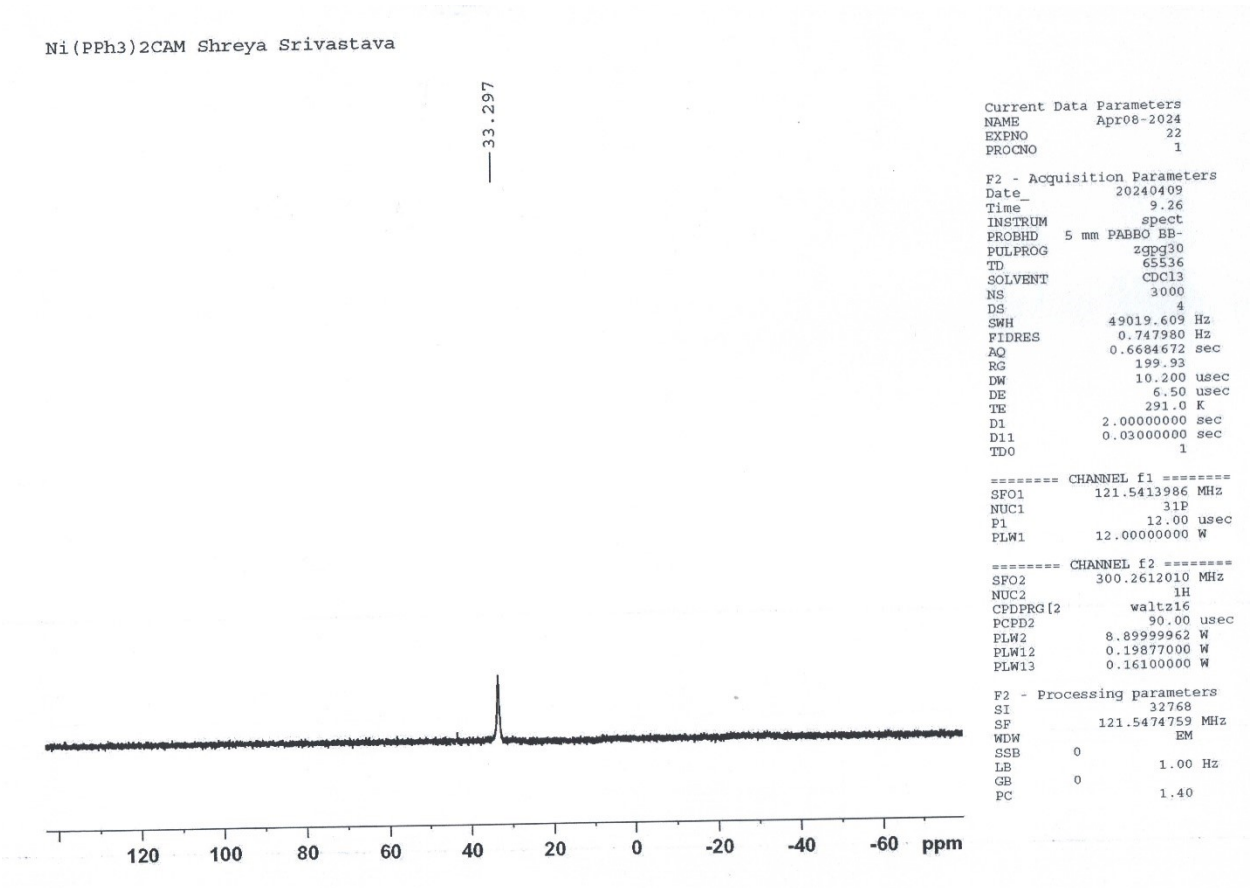

Fig. S12 ^{31}P NMR spectrum of **Ni-3**.

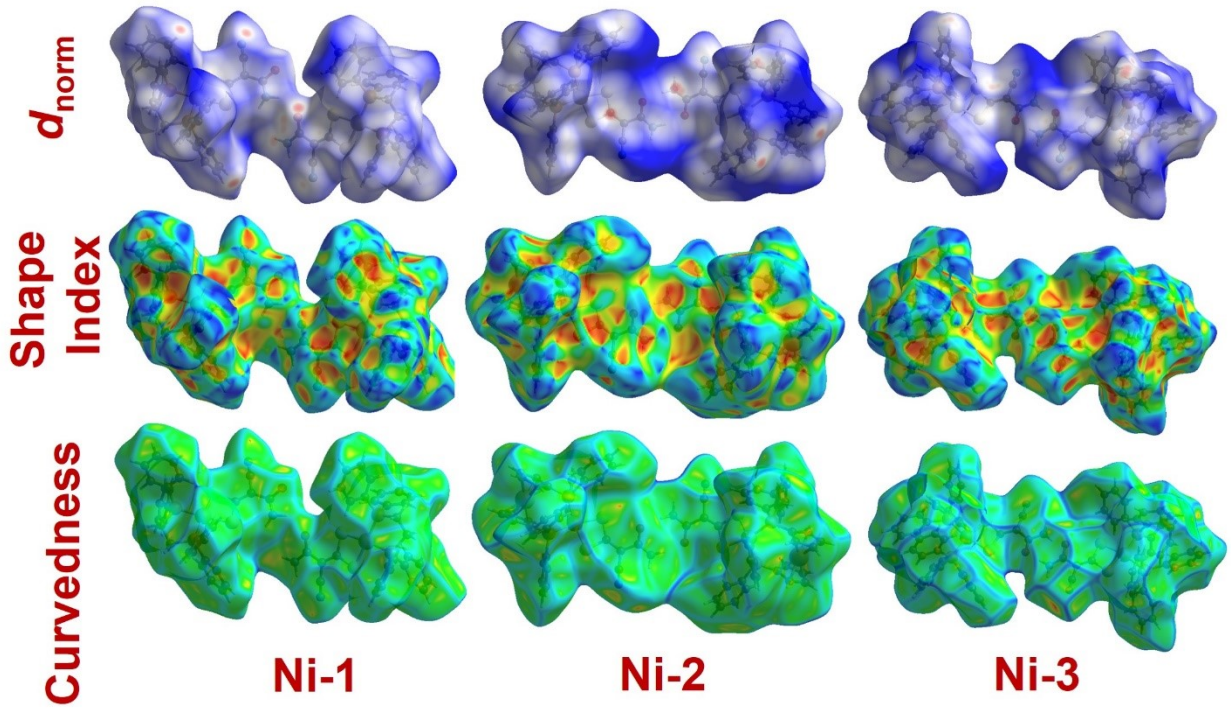

Fig. S13 Results of the Hirshfeld surface analyses for Ni-1, Ni-2 and Ni-3 showing d_{norm}, shape index and curvedness.

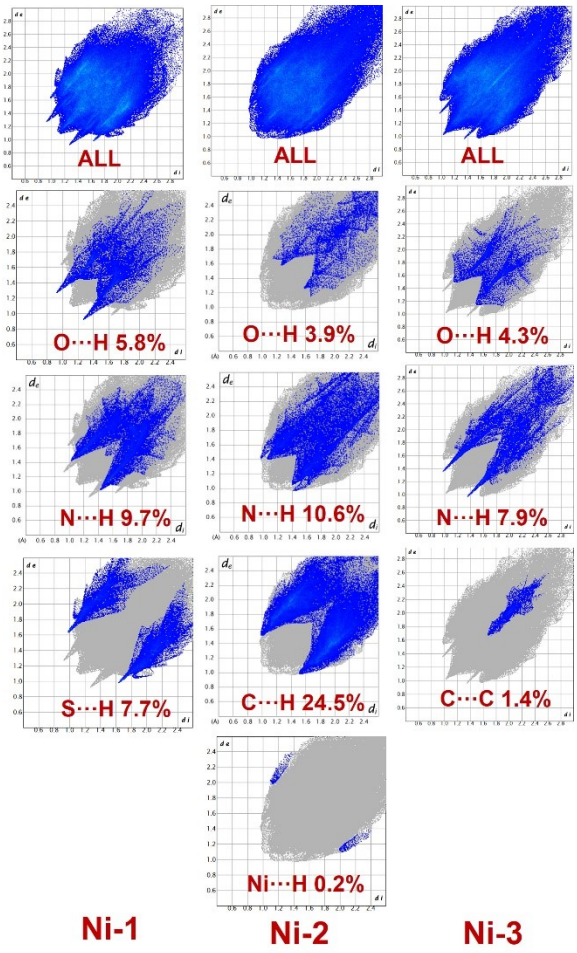

Fig. S14 Total and delineated 2D fingerprint plots for Ni-1, Ni-2 and Ni-3.

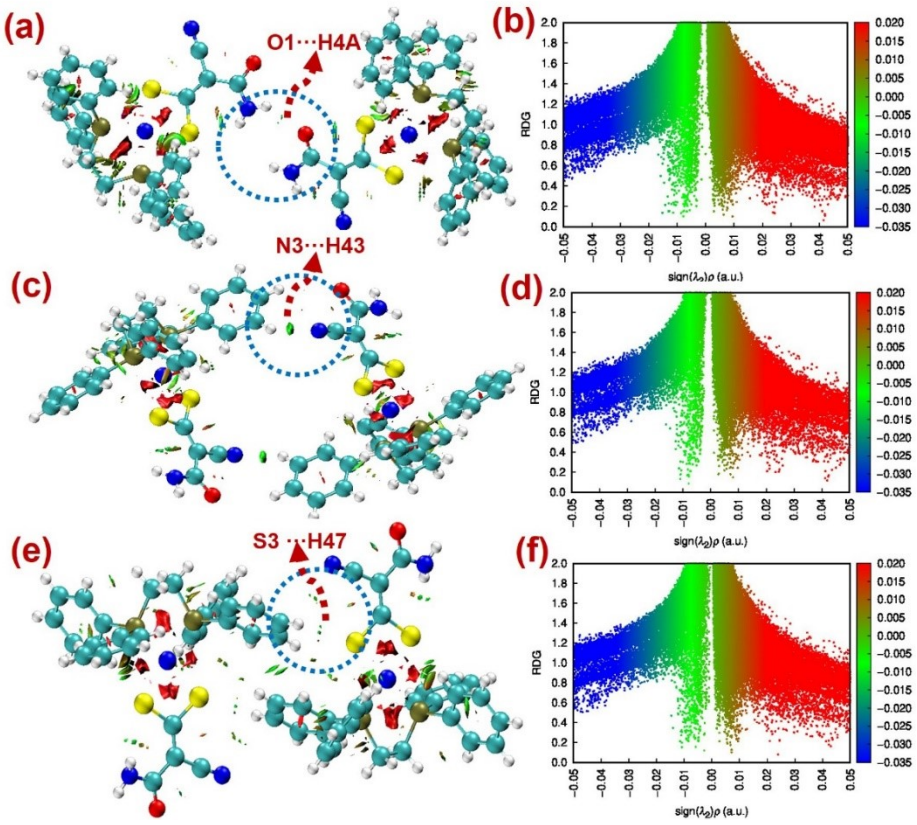

Fig. S15 The intermolecular (a) N-H□□□O=C interactions; (c) intermolecular C≡N□□□H interactions; (e) intermolecular (Ar)C-H□□□S interactions and (b), (d) and (f) as 2D scatter plot for Ni-1 corresponding interactions, respectively.

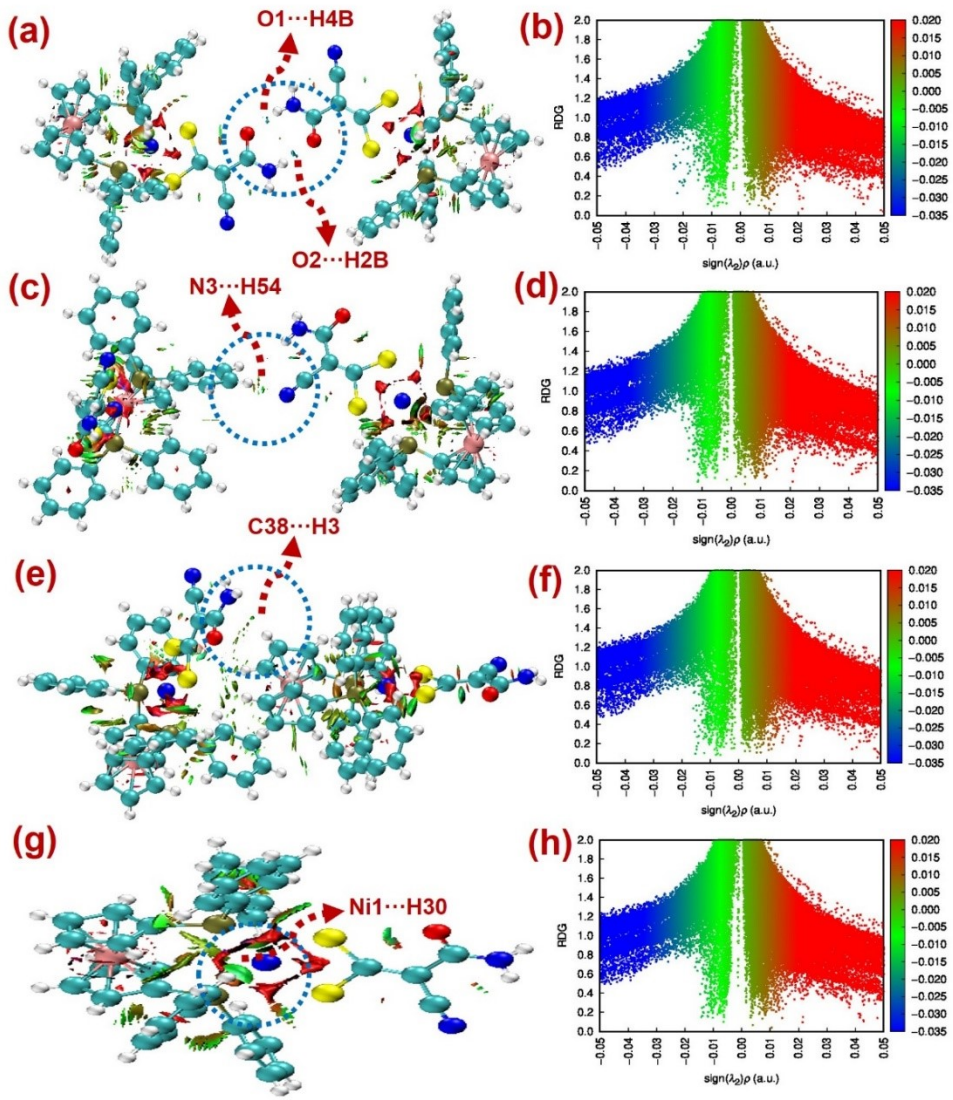

Fig. S16 The intermolecular (a) N-H⋯O=C interactions; (c) intermolecular C≡N⋯H(Ar) interactions; (e) (FcC)H⋯C=O interaction; (g) intramolecular (Ar)C-H⋯Ni anagostic whereas (b), (d), (f) and (h) as 2D scatterplots for the respective interactions in Ni-2.

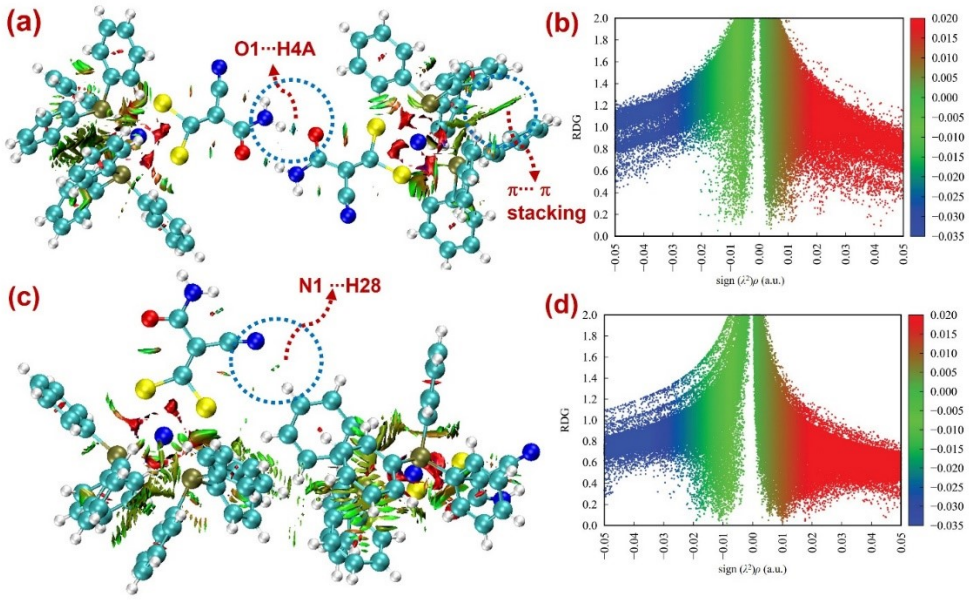

Fig. S17 The intermolecular (a) N-H□□□O=C interactions and π□□□π stacking; (c) intermolecular C≡N□□□H(Ar) interactions; whereas (b) and (d) as 2D scatter plots for the respective interactions in Ni-3.

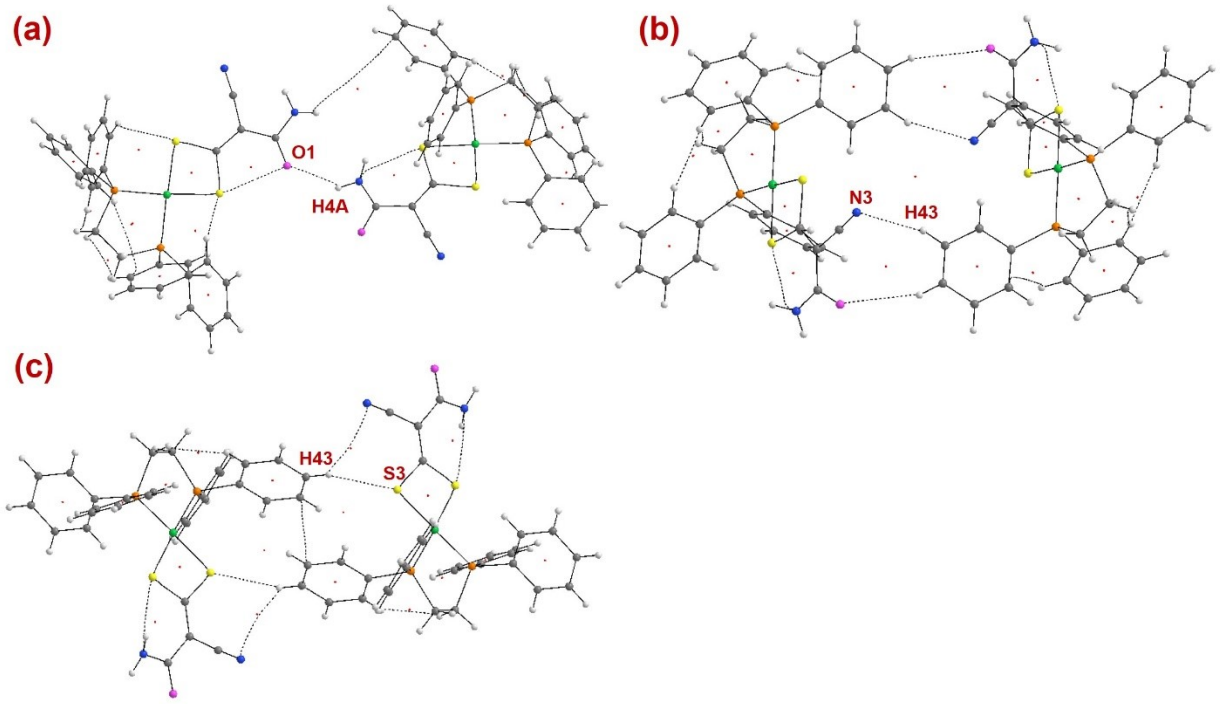

Fig. S18 Quantum Theory of atoms in molecular graphs for (a) N-H□□□O=C; (b) C≡N□□□H and (c) (Ar)C-H□□□S non-covalent interactions in Ni-1

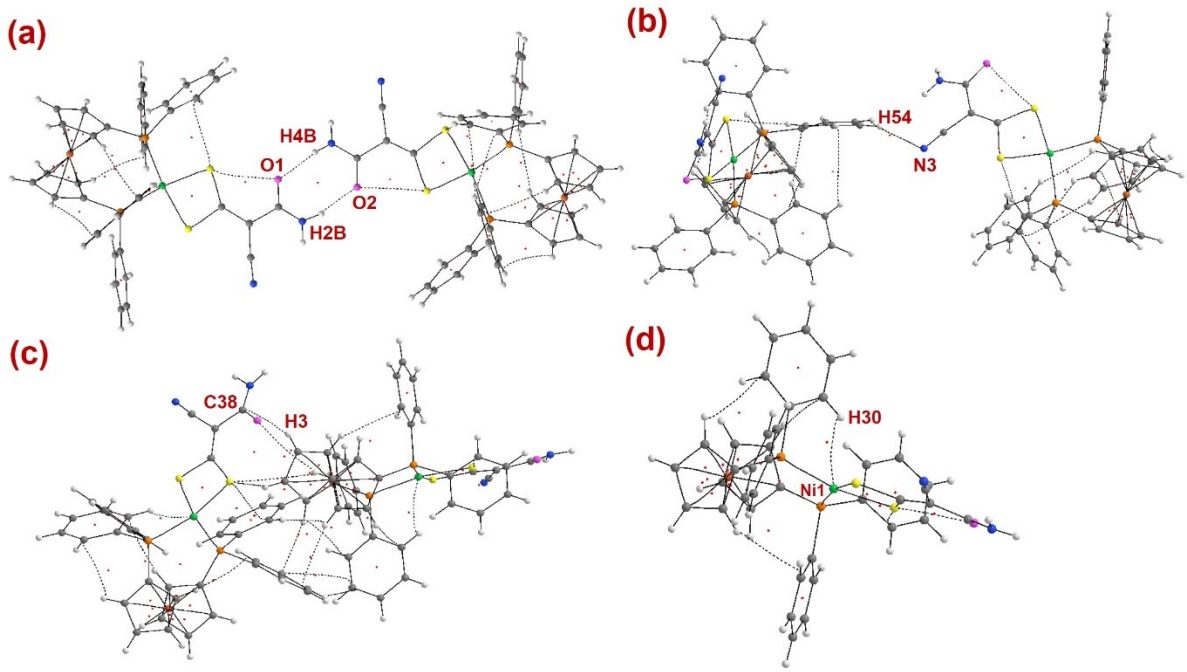

Fig. S19 Quantum Theory of atoms in molecule (QTAIM) images of Ni-2 (a) dimer held by a pair of (a) intermolecular N-H⋯O=C interactions; (b) 1D chain of Ni-2 sustained by C≡N⋯H(Ar) interactions; (c) 1D chain of Ni-2 sustained by (FcC)H⋯C=O interactions and (d) The intramolecular (Ar)C-H···Ni anagostic interaction.

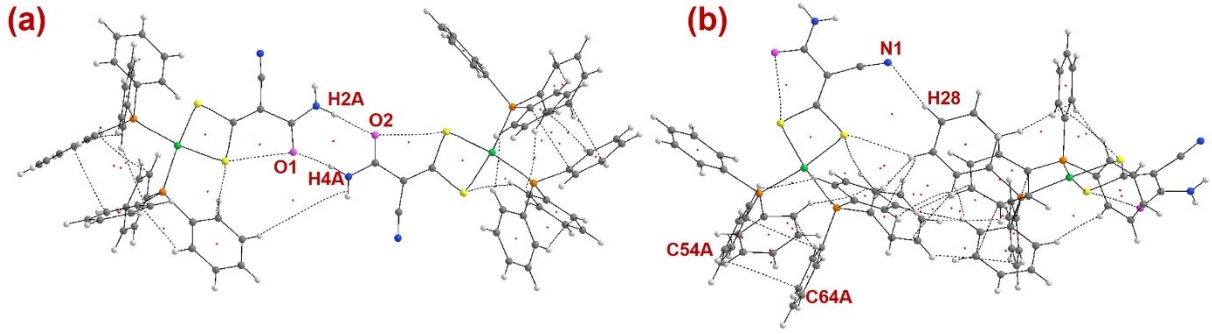

Fig. S20 Quantum Theory of atoms in molecule (QTAIM) images of Ni-3 (a) N-H⋯O=C interactions; (b) C≡N⋯H(Ar) interactions and Intramolecular π⋯π stacking between phenyl rings of PPh_3 ligand.

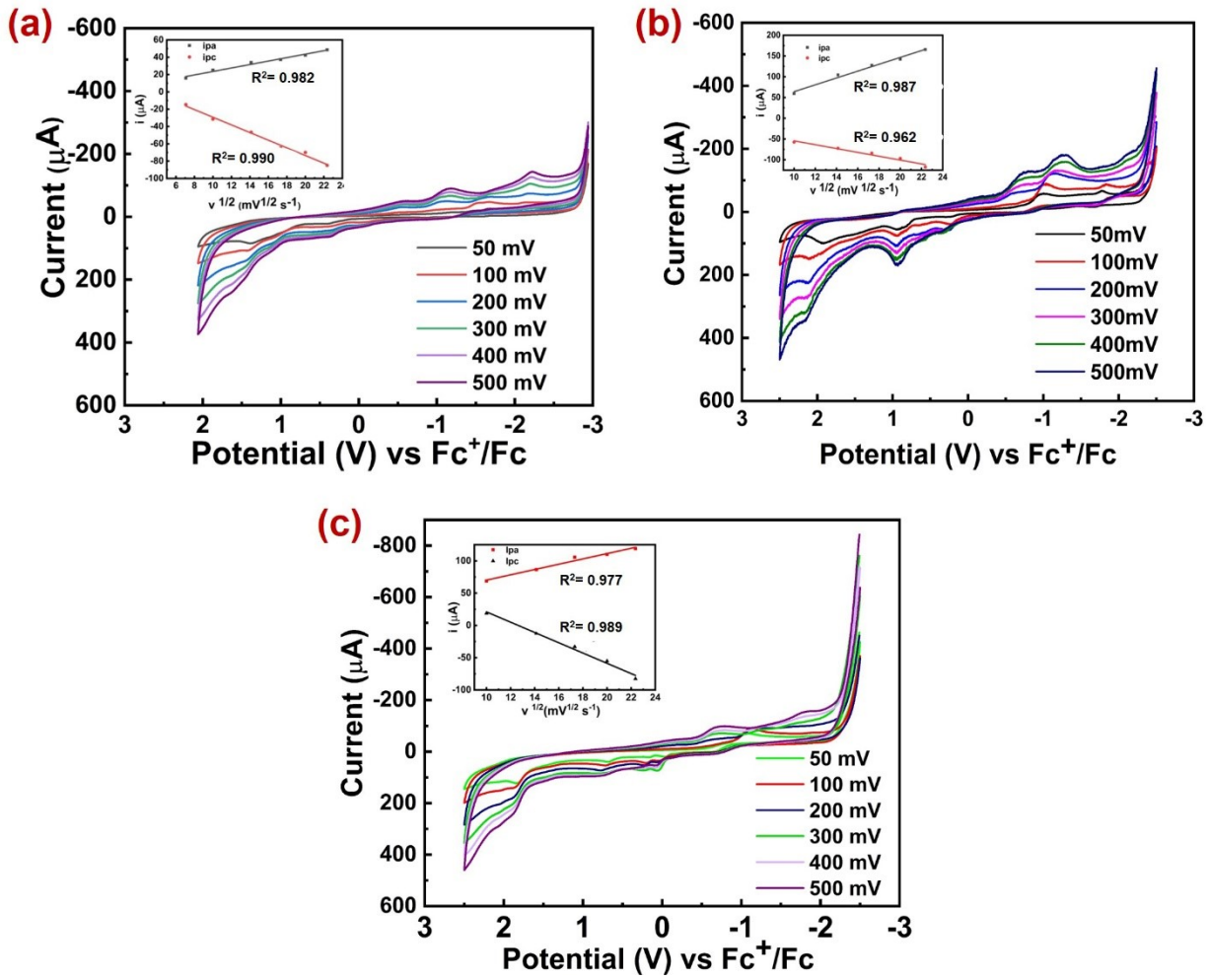

Fig. S21 Cyclic voltammograms ***for*** (a) Ni-1; (b) Ni-2 and (c) Ni-3 recorded in 1 mM acetonitrile solutions at variable scan rates. Insets: Plots of i_{pc} vs. $\nu^{1/2}$. Conditions: 0.1 M TBAP as supporting electrolyte; glassy carbon working electrode (3 mm diameter); platinum wire counter electrode; Ag/AgCl reference electrode; potential vs. Fc^{+}/Fc; 50 to 500 $mV \cdot s^{-1}$ scan rate.

Table S1. Selected geometrical parameters for the complexes.

Ni-1		**Ni-2**		**Ni-3**	
Bond length (Å)		Bond length (Å)		Bond length (Å)	
Ni1-S1	2.2009(11)	Ni1-S1	2.1965(8)	Ni1-S1	2.2090(10)
Ni1-S2	2.1897(10)	Ni1-S2	2.1993(9)	Ni1-S2	2.1878(8)
Ni1-P1	2.1626(11)	Ni1-P1	2.2060(9)	Ni1-P1	2.2293(8)
Ni1-P2	2.1699(10)	Ni1-P2	2.1901(8)	Ni1-P2	2.1972(9)
C27-C28	1.355(10)	C35-C36	1.396(7)	C37-C38	1.374(8)
Bond Angles (°)		Bond Angles (°)		Bond Angles (°)	
∠S1-Ni1-S2	78.96(4)°	∠S1-Ni1-S2	77.94(4)°	∠S1-Ni1-S2	77.62(3)°
∠P1-Ni1-P2	87.87(4)°	∠P1-Ni1-P2	102.43(3)°	∠P1-Ni1-P2	100.31(3)°

Table S2. The selected topographical parameters of inter-molecular interactions computed at bond critical points of interacting atom centres for Ni-1, Ni-2 and Ni-3.

Interaction Type	**ρ**	**$\nabla^2\rho$**	**(ε)**	**H**	**E (kcal·mol^{-1})**
			Ni-1		
O1···H4A	+0.0125	+0.0440	+0.0374	+0.0007	+2.98
N3···H43	+0.0079	+0.0249	+0.0911	+0.0009	+1.38
S3···H47	+0.0097	+0.0327	+0.0842	+0.0014	+1.63
			Ni-2		
O1···H4B	+0.0222	+0.0638	+0.0352	-0.0006	+5.40
O2···H2B	+0.0222	+0.0669	+0.0568	-0.0004	+5.46
N3···H54	+0.0062	+0.0240	+1.4136	+0.0014	+1.03
C38···H3	+0.0058	+0.0258	+3.4506	0.0015	+1.03
Ni1···H30	+0.0123	+0.0433	+1.5455	+0.0009	+2.82
			Ni-3		
O1···H4A	+0.0177	+0.0514	+0.0437	-0.00004	+4.32
O2···H2A	+0.0203	+0.0621	+0.0676	-0.00003	+5.07
N1···H28	+0.0095	+0.0308	+0.0146	+0.00100	+1.75
C54A···C64A	+0.0083	+0.0247	+0.8155	+0.00114	+1.22

Table S3. Experiment results of complex **Ni-1** (1 mM) in TBAP (0.1 M)/MeCN with incremental addition of TFA.

TFA (mM)	i_{cat}/i_p	TOF (s^{-1})	$E_{cat/2}$ (V)	Overpotential (V)
5	3.89	5.89	-1.055	0.239
10	4.70	8.59	-1.058	0.242
15	8.89	30.72	-1.478	0.662
20	11.26	49.27	-1.511	0.695
25	14.49	81.54	-1.557	0.741
30	17.76	122.50	-1.604	0.788
35	20.77	167.46	-1.651	0.835
40	23.49	214.21	-1.752	0.909
45	26.72	277.11	-1.798	0.982
50	28.69	319.50	-1.845	1.029

Table S4. Experiment results of complex **Ni-2** (1 mM) in TBAP (0.1 M)/MeCN with incremental addition of TFA.

TFA (mM)	i_{cat}/i_p	TOF (s^{-1})	$E_{cat/2}$ (V)	Overpotential (V)
5	3.06	3.64	-1.261	0.445
10	5.54	11.94	-1.037	0.221
15	9.57	35.56	-1.15	0.334
20	11.70	53.15	-1.52	0.704
25	15.21	89.77	-1.548	0.732
30	17.40	117.54	-1.584	0.768
35	20.95	170.36	-1.571	0.755
40	24.89	240.42	-1.552	0.736
45	27.27	288.73	-1.604	0.788
50	29.65	341.23	-1.618	0.802

Table S5. Experiment results of complex **Ni-3** (1 mM) in TBAP (0.1 M)/MeCN with incremental addition of TFA.

TFA (mM)	i_{cat}/i_p	TOF (s^{-1})	$E_{cat/2}$ (V)	Overpotential (V)
5	2.79	3.04	-0.971	0.155
10	8.92	30.89	-1.576	0.76
15	12.06	56.44	-1.738	0.922
20	16.33	103.54	-1.803	0.987
25	20.38	161.18	-1.849	1.033
30	23.67	217.41	-1.873	1.057
35	27.00	283.01	-1.896	1.08
40	30.04	350.18	-1.903	1.087
45	33.15	426.59	-1.942	1.126
50	37.42	543.54	-1.971	1.155

Table S6. Electrochemical characteristic properties of complexes Ni-1, Ni-2 and Ni-3 at 500 $mV \cdot s^{-1}$

Complex	E_{pc} (V)	E_{pa} (V)	ΔE_p (V)	E^O (V)	i_{pa}/i_{pc}	D_{cat} ($cm^2 \cdot s^{-1}$)
Ni-1	-1.159	1.181	2.340	0.011	1.292	1.36×10^{-6}
Ni-2	-0.767	0.929	1.696	0.081	1.276	1.28×10^{-5}
Ni-3	-0.699	0.785	1.484	0.043	0.922	4.25×10^{-5}

Table S7. Comparison of overpotentials (**η**) of the synthesized complexes to other recently synthesized Ni(II) complexes

S/No.	Complex	Solvent	Acid (Conc.)	η (mV)	TOF (s^{-1})	Reference
1.	(Ar_4)PNi(II)	CH_3CN	TFA (15 mM)	~880	-	[1]
2.	(F_5Ph)PNi(II)	CH_3CN	TFA (15 mM)	~800	-	[1]
3.	$Ni[P_2S_2C_2(C_6H_4R\text{-}P)_2]$, R= CH_3O	DMF	TFA (15 mM)	1020	802	[2]
4.	$Ni[P_2S_2C_2(C_6H_4R\text{-}P)_2]$, R= CH_3	DMF	TFA (15 mM)	1000	894	[2]
5.	$Ni[P_2S_2C_2(C_6H_4R\text{-}P)_2]$,	DMF	TFA (15 mM)	970	872	[2]

	R= H					
6.	$Ni[P_2S_2C_2(C_6H_4R\text{-}P)_2]$, R= Br	DMF	TFA (15 mM)	910	557	[2]
7.	$Ni[P_2S_2C_2(C_6H_4R\text{-}P)_2]$, R= F	DMF	TFA (15 mM)	950	423	[2]
8.	$[Ni(II)L(L')_2]$ L′ = PPh_3	CH_3CN	TFA (15 mM)	450*	3280	[3]
9.	$[Ni(II)L(L')_2]$ L′ = dppf	CH_3CN	TFA (15 mM)	640*	1050	[3]
10.	$[Ni(II)L(L')_2]$ L′ = dppe	CH_3CN	TFA (15 mM)	1013*	-	[3]
11.	$[BzPy]_2[Ni(mnt)_2]$	CH_3CN	AcOH (170 mM)	388.1	3529.3	[4]
	$[BzPy]_2[Ni(i\text{-}mnt)_2]$	CH_3CN	AcOH (170 mM)	344.1	3425.6	[4]
12.	$[BzPy]_2[Ni(tdas)_2]$	CH_3CN	AcOH (170 mM)	520.1	52476.0	[4]
13	[Ni(bpy)(mp)]	DMF	TFA	580	-	[5]
14	[Ni(dmbpy)(mp)]	DMF	TFA	720	-	[5]
15.	$[(dcpf)Ni(S_2P\{O\}OR]$, R = CH_3	CH_3CN	TFA (120 mM)	620	1243.83	[6]
16.	$[(dcpf)Ni(S_2P\{O\}OR]$, R = CH_3CH_2	CH_3CN	TFA (120 mM)	580	1046.54	[6]
18.	$[(dcpf)Ni(S_2P\{O\}OR]$, R = Ph	CH_3CN	TFA (120 mM)	710	1331.71	[6]
19.	$[(dcpf)Ni(S_2P\{O\}OR]$, R = 4-MeC_6H_4	CH_3CN	TFA (120 mM)	670	2545.29	[6]
20.	$[(dcpf)Ni(S_2P\{O\}OR]$, R = $PhCH_2$	CH_3CN	TFA (120 mM)	600	1899.03	[6]
21.	$[(dcpf)Ni(S_2P\{O\}OR]$, R = $PhCH_2CH_2$	CH_3CN	TFA (120 mM)	560	1191.37	[6]
22.	**Ni-1**	CH_3CN	TFA (50 mM)	1029	319	This study
23.	**Ni-2**	CH_3CN	TFA (50 mM)	802	341	This study
24.	**Ni-3**	CH_3CN	TFA (50 mM)	1155	543	This study

*The $E_{1/2}$ value is calculated from CV following this

References

1. S. Xue, X. Lv, N. Liu, Q. Zhang, H. Lei, R. Cao, F. Qiu, *Inorg. Chem*., 2023, **62,** 1679-1685.
2. L. Chen, T. Li, B. Xie, C. Lai, R.W. Ji, J.Y. He, D.L. Zhang, *Catal. Sci. Technol*., 2023, **13**, 3655-3666.
3. A. Mishra, G.K. Mishra, Anamika, N. Singh, R. Kant, K. Kumar, *Dalton Trans.,* 2024, **53** ,1680-1690.
4. Z. Niu, L. Yang, Y. Xiao, M. Xue, J. Zhou, L. Zhang, C. Ni, *Electrocatalysis*, 2022, **13,** 230-241.
5. F. Kamatsos, K. Bethanis, C.A. Mitsopoulou, *Catalysts,* 2021, **11**, 401.

6. D.L. Zhang, C.L. Deng, B. Xie, Y.L. Li, C. Lai, W.Y. Mou, J. Wang, *Appl. Organomet. Chem.,* 2020, **34,** e5261.